Environmental Research 215 (2022) 114223

Contents lists available at ScienceDirect

Environmental Research

journal homepage: www.elsevier.com/locate/envres

Needle age and precipitation as drivers of Hg accumulation and deposition in coniferous forests from a southwestern European Atlantic region

Melissa Méndez-López [a,b,*], Antía Gómez-Armesto [a,b], Cristina Eimil-Fraga [c], Flora Alonso-Vega [a,b], Roque Rodríguez-Soalleiro [c], Esperanza Álvarez-Rodríguez [d], Manuel Arias-Estévez [a,b], Juan Carlos Nóvoa-Muñoz [a,b]

[a] Universidade de Vigo, Departamento de Bioloxía Vexetal e Ciencia do Solo, Área de Edafoloxía e Química Agrícola, Facultade de Ciencias, As Lagoas s/n, 32004, Ourense, Spain
[b] Campus da Auga, Universidade de Vigo, Laboratorio de Tecnoloxía e Diagnose Ambiental, Rúa Canella da Costa da Vela 12, 32004, Ourense, Spain
[c] Unidad de Gestión Ambiental y Forestal Sostenible, Escuela Politécnica Superior de Ingeniería, Universidade de Santiago de Compostela, Rúa Benigno Ledo s/n, 27002, Lugo, Spain
[d] Departamento de Edafología y Química Agrícola, Escuela Politécnica Superior de Ingeniería, Universidade de Santiago de Compostela, Rúa Benigno Ledo s/n, 27002, Lugo, Spain

ARTICLE INFO

Keywords:
Pinus pinaster
Litterfall
Bioindicator
Atmospheric pollutants
Foliage
Aboveground biomass

ABSTRACT

Vegetation and climate are critical in the biogeochemical cycle of Hg in forest ecosystems. The study assesses the influence of needle age and precipitation on the accumulation of Hg in needle biomass and its deposition by litterfall in thirty-one pine plantations spread throughout two biogeographical regions in SW Europe. Well-developed branches of *Pinus pinaster* were sampled and pine needles were classified according to 4 age classes (y_0, y_1, y_2, y_3). The concentration of total Hg (THg) was analyzed in the samples and Hg content in needle biomass and its deposition by litterfall were estimated. The concentration of total Hg (THg) increased with needle age ranging from 9.1 to 32.7 μg Hg kg^{-1} in the youngest and oldest needles, respectively. The rate of Hg uptake (Hg_R) three years after needle sprouting was 10.2 ± 2.3 μg Hg kg^{-1} yr^{-1}, but it decreased with needle age probably due to a diminution in photosynthetic activity as needles get older. The average total Hg stored in needle biomass (Hg_{Wt}) ranged from 5.6 to 87.8 mg Hg ha^{-1}, with intermediate needle age classes (y_1 and y_2) accounting for 70% of the total Hg stored in the whole needle biomass. The average deposition flux of Hg through needle litterfall (Hg_{Lt}) was 1.5 μg Hg m^{-2} yr^{-1}, with the y_2 and y_3 needles contributing most to the total Hg flux. The spatial variation of THg, Hg_{Wt} and Hg_{Lt} decreased from coastal pine stands, characterized by an oceanic climate, to inland pine stands, a feature closely related to the dominant precipitation regime in the study area. Climatic conditions and needle age are the main factors affecting Hg accumulation in tree foliage, and should be considered for an accurate assessment of forest Hg pools at a regional scale and their potential consequences in the functioning of terrestrial ecosystems.

1. Introduction

Mercury is a global pollutant derived from both natural and anthropogenic sources (Driscoll et al., 2013), whose progressive accumulation in different compartments of the biosphere during the last decades have triggered impacts on wildlife and human health (UN Environment, 2018; Zhang et al., 2021).

Trees are considered the largest Hg pool in forest ecosystems after soils (Yang et al., 2018), with foliage being responsible for the uptake of 49% of the global total Hg assimilated by vegetation (Zhou and Obrist, 2021). Tree foliage uptakes mostly gaseous elemental Hg, Hg(0), by stomata (Laacouri et al., 2013) and non-stomata routes (Arnold et al., 2018), and it is afterward accumulated in leaves/needles along their lifetime to be finally transferred to soil surface through litterfall as a result of foliage shedding (Wang et al., 2019a; Zhou and Obrist, 2021; Zhou et al., 2021). Litterfall was proved to be the main pathway of Hg

* Corresponding author. Universidade de Vigo, Departamento de Bioloxía Vexetal e Ciencia do Solo, Área de Edafoloxía e Química Agrícola, Facultade de Ciencias, As Lagoas s/n, 32004, Ourense, Spain.
E-mail address: memendez@uvigo.es (M. Méndez-López).

https://doi.org/10.1016/j.envres.2022.114223
Received 25 May 2022; Received in revised form 29 July 2022; Accepted 24 August 2022
Available online 5 September 2022

deposition to soils in forest ecosystems (Juillerat et al., 2012; Wang et al., 2016a; Wright et al., 2016; Gerson et al., 2017; Zhou et al., 2020), although recent findings showed that the direct deposition of gaseous elemental Hg can triple the amount of Hg deposited through litterfall in forested areas (Obrist et al., 2021).

Needles of coniferous species had been widely used to monitor atmospheric contaminants such as Hg due to their scavenging properties, longer lifespan and a greater surface area per volume of foliage than broadleaf deciduous species (Witt et al., 2009; Obrist et al., 2012; Juillerat et al., 2012; Hutnik et al., 2014). Thus, Hg is progressively accumulated in needle/leaf tissues as the exposure period and/or foliar age increase (Lyapina, 2018; Turkyilmaz et al., 2018; Wohlgemuth et al., 2020; Woś et al., 2021). Since Hg accumulated in needles is finally transferred to soil surface through litterfall, an estimate of the amount of Hg stored in foliage can be used to assess how much Hg can potentially reach the soil surface (Zhou and Obrist, 2021).

Besides vegetation, climate characteristics have been reported to be a powerful driver of Hg storage in forest soils (Wang et al., 2019a). Thus, it has been shown that in coastal areas, common events of occult deposition (fog and dew), rainfall and maritime winds contribute to the transport of Hg (Hg^{2+} bound to sea salt aerosols) from the ocean to nearshore forests which are potential sinks for Hg (Coale et al., 2018; Peckham et al., 2019). In addition, climate may affect Hg fate in forest ecosystems by modifying soil organic C dynamics (Hararuk et al., 2013), promoting the succession of different tree species (Richardson and Friedland, 2015), or altering Hg deposition pathways (Blackwell et al., 2014; Yang et al., 2019).

In southern Europe, forests are extremely vulnerable to disturbances due to climate change (Forzieri et al., 2021). Considering the worst scenario, an increase of 4–6 °C in the mean annual temperature and a 15–20% decrease in mean annual precipitation is expected for 2080 (EEA, 2017). Depending on the extent of these predictions, the ability of foliar tree biomass to accumulate atmospheric Hg could be strongly modified at different spatial scales. Recently, foliar Hg uptake fluxes were quantified in several tree species from central to northern Europe (Wohlgemuth et al., 2020). Unfortunately, Hg data in vegetation from southern European regions, where direct and indirect impacts of climate change are expected to be more pronounced, are scarce.

As mentioned above, the influence of leaf age of different tree species and climate conditions on the presence of Hg in forest ecosystems were assessed separately. Although scarce, there are also studies on the effect of fog and precipitation on the transport of Hg to coastal areas. However, one of the new contributions of this work is to address these factors (needle age and climate conditions) simultaneously. Also as novelty, the present study goes further than assessing how these factors affect to Hg concentration in pine needles, extending its assessment to estimate Hg accumulated in total needle biomass and Hg deposition to the soil surface by needle litterfall. For this purpose, several stands of maritime pine (*Pinus pinaster*, Aiton) spread across Galicia (NW Iberian Peninsula), a transition area among the Eurosiberian and the Mediterranean biogeographic regions in southwest Europe, were selected. The variation of Hg concentration and storage in needles, and Hg deposition through litterfall was geographically modeled as a function of precipitation. The results obtained would contribute to new insights into the fate of Hg in forest ecosystems from background areas of SW Europe, where empirical data are scarce and the predictions of the European Monitoring and Evaluation Programme (EMEP) have a high degree of uncertainty.

2. Material and methods

2.1. Study area, sampling sites and needle collection

The study was carried out in Galicia, a territory of about 30.000 km^2 located in the western corner of the Iberian Peninsula (Fig. 1). Galicia is

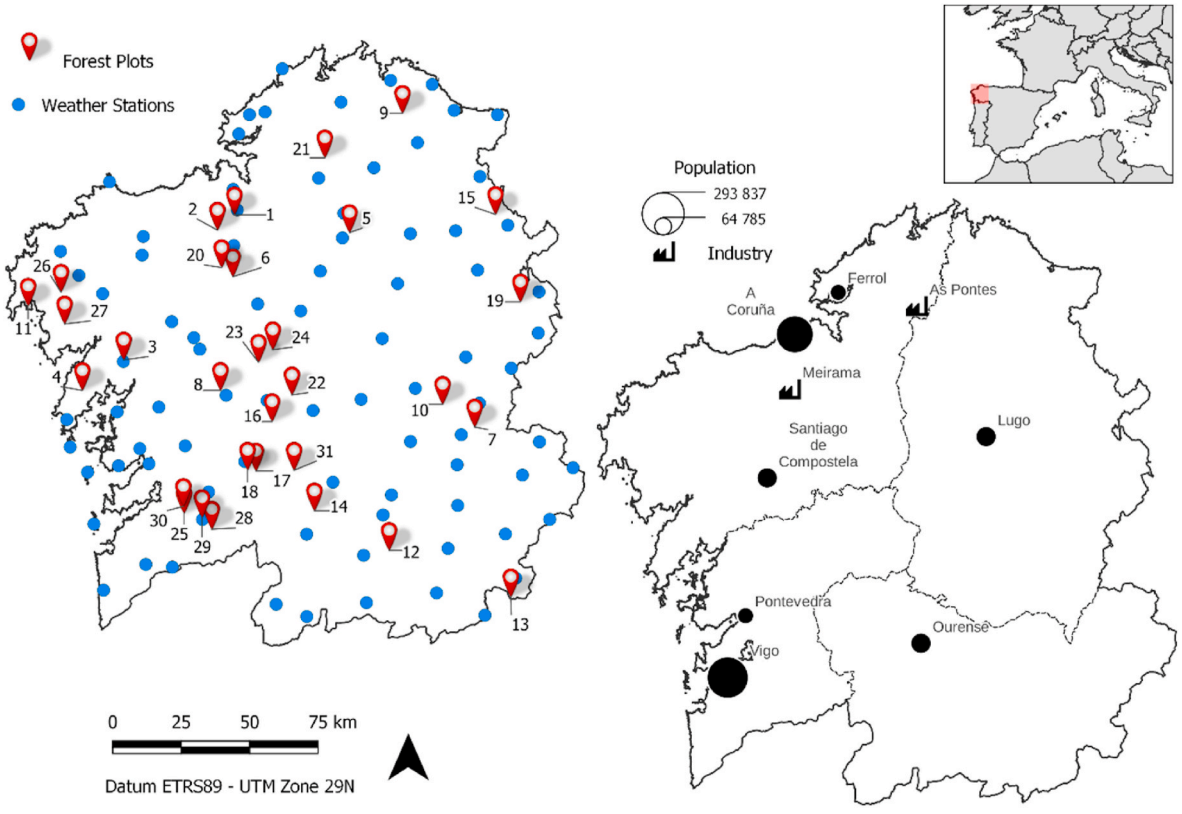

Fig. 1. Location of the study area (Galicia, NW Iberian Peninsula) in southwest Europe including the main cities and the coal-fired power plants (right). Distribution of the 31 *Pinus pinaster* forest stands (red labels) and the weather stations considered (blue labels) throughout the study area (left). (For interpretation of the references to colour in this figure legend, the reader is referred to the Web version of this article.)

divided into the Eurosiberian and the Mediterranean biogeographic regions with a marked transition of climatic characteristics from the west to the east. The northern and western area (the Eurosiberian) is a coastal zone strongly influenced by oceanic cold fronts resulting in total annual rainfall up to 2300 mm, whereas the inland area (the Mediterranean) is characterized by a lesser maritime influence and rainfall ranging from 700 to 1500 mm yr^{-1} (Souto et al., 2003). The mean annual temperature is about 12 °C, although it varies slightly between coastal and inland areas. The climax vegetation in the study area is deciduous broadleaf forest dominated by *Quercus robur* (L.). However, coniferous maritime pine (*Pinus pinaster*, (Ait.)) has progressively spread as a result of the afforestation process carried out in the study area, until occupying over 200.000 ha (Picos and Rodríguez-Soalleiro, 2019). In the pine forest stands, the understory is shrubs (*Ulex* sp., *Erica* sp., *Calluna vulgaris*), fern (*Pteridium aquilinum*), creeping ivy (*Hedera helix*), wild blackberry (*Rubus ulmifolius*) and different annual and biannual herbaceous species.

Thirty-one maritime pine forest stands composed of individuals of similar age (11–13 years old) were selected throughout Galicia for this study (Fig. 1), covering an altitude range from 80 to 900 m a.s.l (Table S1). The pine stands were classified as inland or coastal stands according to the biogeographic region they come from (Mediterranean *vs* Eurosiberian), but also factors such as the distance to the coastline, mean annual precipitation as well as stands location with regard to the prevailing winds throughout the year were considered. Pine stands characterization, pine needles sampling (performed in October 2009) and needle age class assignment were described in detail elsewhere (Eimil-Fraga et al., 2015a, b). Briefly, in each stand, three dominant pine trees were selected and a well-developed branch oriented in the direction of the prevailing winds (mainly from the SW) was removed from the upper third of the crown of each tree. From each branch, all the needles were collected and classified by age classes as follows: 0 year-old needles (y_0; sprouted during the sampling year, 2009), 1 year-old needles (y_1; sprouted during 2008), 2 year-old needles (y_2; sprouted during 2007) and 3 year-old needles (y_3; sprouted in 2006). The sampling was carried out at the end of the growing season in order to ensure that needles of each age class showed the maximum Hg content (Demers et al., 2013).

The sampling procedure resulted in 294 needle batches corresponding to a combination of stands (31), trees (3 per stand), branches (1 per tree) and age classes (from 2 to 4 depending on the tree branch and stand). All needle batches were identified in the field, stored in polyethylene zip bags and transported to the laboratory in a portable refrigerator (4 °C). Each needle batch was separated into 3 subsamples for different purposes. The first set of subsamples set was oven-dried to a constant weight (65 °C for 48 h) to average the dry weight of a single needle. A second set was air-dried to determine the main morphological needle characteristics by each age class such as length, thickness, width, leaf area, etc. (Eimil-Fraga et al., 2015a). The third set of subsamples was freeze-dried, ground in a grinder using a mesh diameter of 0.5 mm (POLYMIX PX-MFC) and milled in a mechanical agate mortar (Retsch RM200) followed by analysis for total Hg. During needle collection and their preparation for Hg analysis, polyvinyl gloves were used to avoid sample contamination whereas the grinder and the mortar were cleaned with diluted HCl and distilled water to minimize cross-contamination among samples.

2.2. Total Hg determination

The determination of the total Hg (THg) content in the milled needle samples was conducted using a Milestone tri-cell Direct Mercury Analyzer (DMA-80). The analytical method is based on thermal combustion, amalgamation and atomic absorption spectroscopy (U.S. EPA, method 7473). All the samples were measured twice, weighing about 100 mg and repeating the measurement when the coefficient of variation among duplicates exceeded 10%. In terms of quality assurance and control purposes (QA/QC), the accuracy of Hg determination was assessed using the standard reference material NIST 1547 (peach leaves) with Hg certified values of 31 ± 7 μg kg^{-1}. Standard reference material was measured at the beginning of each analytical run and every twenty sample measurements, obtaining a recovery percentage of 98.6% (average 30.6 ± 0.5 μg kg^{-1}; n = 40). The detection limit of the method was 0.43 μg kg^{-1} considering three times the standard deviation of the mean blank concentrations and an average sample mass of 0.100 g.

2.3. Calculations

2.3.1. Mercury accumulation rate in needles

Mercury accumulation rate (Hg_R) was assumed as the slope of the linear regression fit (least square method) of Hg concentrations in needles with exposure time. Values of Hg_R were calculated for each stand and needle age interval. Assuming that at the beginning of needle sprout THg is negligible, regression was forced to zero and Hg_R for y_0 needles resulted from the representation of THg concentrations in the sampling year (y_0). Estimation of Hg_R in y_1 needles was calculated representing their THg in the present (y_1) and the preceding growing year (y_0) without forcing the regression to zero. The same procedure was followed for y_2 and y_3 needles (if they were present). A total Hg accumulation rate (Hg_{Rt}) was also calculated for each stand taking into account THg concentrations in y_0, y_1 and y_2 needles, and forcing the regression through zero.

2.3.2. Mercury stored in needle biomass

Before estimating the amount of Hg stored in the needle biomass, total needle biomass (W_{tn}), in Mg ha^{-1}, was calculated for each stand using equation (1) (Hevia et al., 2017).

$$W_{tn} = 0.015 \cdot d^{2.574} \cdot CR^{2.617} \quad (1)$$

This approach is based on tree diameter at breast height (d) and crown ratio (CR) and is adapted to the species (*Pinus pinaster*) and area under study. Both parameters (d and CR) were measured in all the trees present within a representative plot of 20 × 30 m established in each of the 31 studied stands.

The distribution of needle biomass by age class (W_x, in Mg ha^{-1}), where the subscript x represents the needle age class, was estimated considering the dry weight percentage of each needle age class with regard to total needle biomass (W_{tn}). The results were averaged per stand based on the three sampled branches (Online Data Resource).

Mercury accumulated in the biomass of each needle age class (Hg_{Wx}, in mg Hg ha^{-1}), with x ranging from 0 to 3, was calculated by multiplying the Hg concentration by the needle biomass of the corresponding age class (Online Data Resource). For each stand and needle age class, Hg_{Wx} was averaged from the results obtained in needles from the three branches collected. The sum of the averages of Hg_{Wx} (i.e., $Hg_{W0} + Hg_{W1} + Hg_{W2} + Hg_{W3}$) represents the Hg accumulated in the total needle biomass for each pine stand (Hg_{Wt}).

2.3.3. Mercury deposition through litterfall

The annual flux of litterfall (L_x) was estimated, on an areal basis, considering needle survival rate (S_x) and needle biomass (W_x) for each age class as indicated in equation (2) (Eimil-Fraga et al., 2015b).

$$L_x = \frac{W_x}{S_x} \cdot (S_{x-1} - S_x) \quad (2)$$

where L_x is the flux of litterfall comprised by needles of the age class x (in Mg ha^{-1} yr^{-1}), W_x is the needle biomass of the age class x, S_x is the needle survival rate of age class x and S_{x-1} is the survival rate of the previous age class. Values for needle survival (S in eq. (2)) are expressed as ratios of unity, assuming that S_0 (the survival rate of needles sprouted in the sampling year, y_0) is 1 which represents 100% of needle survival. Total litterfall flux for each stand (L_t) was calculated considering the sum of the averaged values of L_x obtained for each needle age class (i.e., L_0 +

$L_1 + L_2 + L_3$). Details of this calculation are shown in Online Data Resource.

Mercury deposition through litterfall was estimated for each needle age class (Hg_{Lx}) by multiplying the Hg concentration in needles of age x by the litterfall flux of needles with the same age, with x varying from 0 to 3 (Online Data Resource). For a given stand, Hg deposition through the litterfall of each needle age class was averaged with the values obtained in the samples collected from the three branches selected per tree. For an individual stand, total Hg deposited through litterfall (Hg_{Lt}) was considered the sum of the averaged values of Hg_{Lx} obtained for each needle age class (i.e., $Hg_{L0} + Hg_{L1} + Hg_{L2} + Hg_{L3}$).

2.4. Meteorological data and mapping

Meteorological data were obtained from Meteogalicia (Meteogalicia.gal, 2021), a public Agency dependent on the Autonomous Government of Galicia for the regional weather forecast. This Agency collects and provides meteorological parameters, on a monthly basis, from different georeferenced weather stations (Fig. 1). For this study, total annual rainfall (L m^{-2}) was calculated as the sum of the monthly precipitation registered from 35, 52, 79 and 81 weather stations for the years 2006, 2007, 2008 and 2009, respectively. In the abovementioned years, total rainfall was also calculated for winter (January–March), spring (April–June), summer (July–September) and autumn (October–December) (see Online Data Resource for additional details).

The spatial variation of Hg descriptors (total Hg concentration in needles, Hg accumulated in needle biomass and Hg deposited through litterfall) was modeled using QGIS Geographic Information System (QGIS.org, 2021) by applying the inverse distance weighting (IDW) method. In addition, precipitation and mean annual temperature in the sampling stands were also estimated by IDW. During the interpolation, sampling points are weighted and their influence over unknown points decreases as the distance among them increases. For proper IDW application, sampling points must be representative of the area studied as IDW assumes that nearby locations are more likely to have similar values (Fortin and Dale, 2005; Olaya, 2012) and estimated values will be within the measured concentration range. Weather stations and forest stands that are shown in Fig. 1 were assumed to be representative of the study area.

2.5. Statistical analyses

Descriptive and statistical analyses were carried out using IBM SPSS Statistics 25 for Windows. Non-parametrical statistical tests were used as most of the variables measured and calculated do not follow a normal distribution. A Kruskal-Wallis test (H) was performed to assess needle age class as an influencing factor on Hg concentration, Hg accumulation in needle biomass and Hg deposition through litterfall, whereas a Mann-Whitney test (U) was applied to ascertain if the inland or coastal location of stands influenced in the parameters related to Hg. Finally, Spearman correlations (ρ) were used to explore relationships among different parameters. For all tests, statistical significance was considered when $p < 0.05$.

3. Results

3.1. Total Hg in needles: concentrations and accumulation rates

The mean concentration of total Hg (THg) for *Pinus pinaster* needles in all stands was 21 ± 11 μg kg^{-1}, with the range 4.3–50.6 μg kg^{-1} (n = 294). Total Hg in needles showed a clear increase with age (Table 1) confirmed by a Kruskal-Wallis test assessing needle age class as a factor (H = 214.1; p = 0.000; n = 294). The lower mean THg concentration corresponded to the needles sprouted during the sampling year (y_0) with 9.1 ± 2.8 μg kg^{-1}, varying between 4.9 μg kg^{-1} (stand 24) and 15.0 μg kg^{-1} (stand 11). Table S2 shows mean values for THg by needle age class and stand. Mean THg concentrations for y_1 needles (22.1 ± 5.8 μg kg^{-1}) were more than twice those for y_0, ranging from 12.1 μg kg^{-1} (stand 13) to 34.8 μg kg^{-1} (stand 11). For y_2 needles, the average THg increased up to 29.9 ± 6.0 μg kg^{-1}, ranging between 19.5 and 43.3 μg kg^{-1} in stands 13 and 26, respectively. Although y_3 needles (sprouted in 2006) were present in few stands, they showed the highest mean concentration of THg with 32.7 ± 8.4 μg kg^{-1} as well as the widest range of THg among stands, varying from 20.9 to 47.5 μg kg^{-1} in stands 15 and 9, respectively (Table S2).

Total Hg in pine needles also showed noticeable differences among stands for each age class assessed (Table S2), resulting in a spatial variation of THg depicted in Fig. 2. For the same age class, THg in needles decreased from stands close to the coast (at the west and north of Galicia) to inland areas. This diminution of THg in pine needles along a coastal-inland gradient becomes more evident in older needles. For example, y_3 needles had the highest values (above 35 μg kg^{-1}) in the southwest and far north of the study area (Fig. 2).

Mean values for Hg accumulation rates (Hg_R) in pine needles, considered as a net uptake of atmospheric Hg(0), were 9.1, 13.0, 8.1 and 4.1 μg Hg kg^{-1} yr^{-1} for y_0, y_1, y_2 and y_3 needles, respectively (Table S3). The Kruskal-Wallis test indicated that values of Hg_R differed significantly with needle age class (H = 27.7; p = 0.000; n = 92) with the younger needles (y_0 and y_1) showing the highest Hg accumulation rates. According to the distribution of Hg_R among the different needle age

Table 1
Mean ± standard deviation and range (between brackets) of total Hg concentration and storage in needles, Hg flux through litterfall and Hg accumulation rates in coastal (n = 18) and inland (n = 13) pine stands according to age classes y_0, y_1, y_2 and y_3 (the sprouting year of each needle age class is presented in brackets).

Location		Needle age class			
		y_0 (2009)	y_1 (2008)	y_2 (2007)	y_3 (2006)
Total Hg concentration (μg kg^{-1})	Coastal	10.6 ± 2.7 (5.6–15.0)	24.7 ± 5.6 (16.6–34.8)	29.9 ± 6.0 (19.5–43.3)	32.7 ± 8.4 (20.9–47.5)
	Inland	7.1 ± 1.4 (4.9–9.5)	18.5 ± 4.0 (12.1–25.4)	27.6 ± 5.6 (19.5–40.2)	27.0 ± 5.8 (20.9–36.8)
Hg stored in needle biomass (mg ha^{-1})	Coastal	7.4 ± 4.9 (2.1–18.5)	19.6 ± 12.1 (4.2–41.8)	14.4 ± 9.7 (0.5–35.8)	7.5 ± 3.1 (1.9–10.9)
	Inland	2.0 ± 1.5 (0.8–5.9)	7.2 ± 4.6 (3.4–19.1)	6.4 ± 6.9 (1.0–27.7)	2.8 ± 2.2 (0.2–6.1)
Hg deposited through litterfall (μg m^{-2})	Coastal	0.04 ± 0.08 (0.00–0.24)	0.25 ± 0.23 (0.02–0.82)	1.36 ± 1.83 (0.00–7.27)	1.63 ± 1.18 (0.16–3.20)
	Inland	0.00 ± 0.00 (0.00–0.02)	0.09 ± 0.09 (0.01–0.29)	0.30 ± 0.19 (0.06–0.67)	0.40 ± 0.64 (0.00–1.81)
Hg accumulation rate (μg kg^{-1} yr^{-1})	Coastal	10.6 ± 2.7 (5.6–15.0)	14.1 ± 4.0 (7.0–22.4)	7.3 ± 2.0 (3.7–10.4)	6.7 ± 2.6 (3.0–10.4)
	Inland	7.1 ± 1.4 (4.9–9.5)	11.4 ± 3.0 (6.3–16.3)	9.1 ± 3.1 (5.6–14.7)	1.2 ± 3.2 (-4.2-5.8)

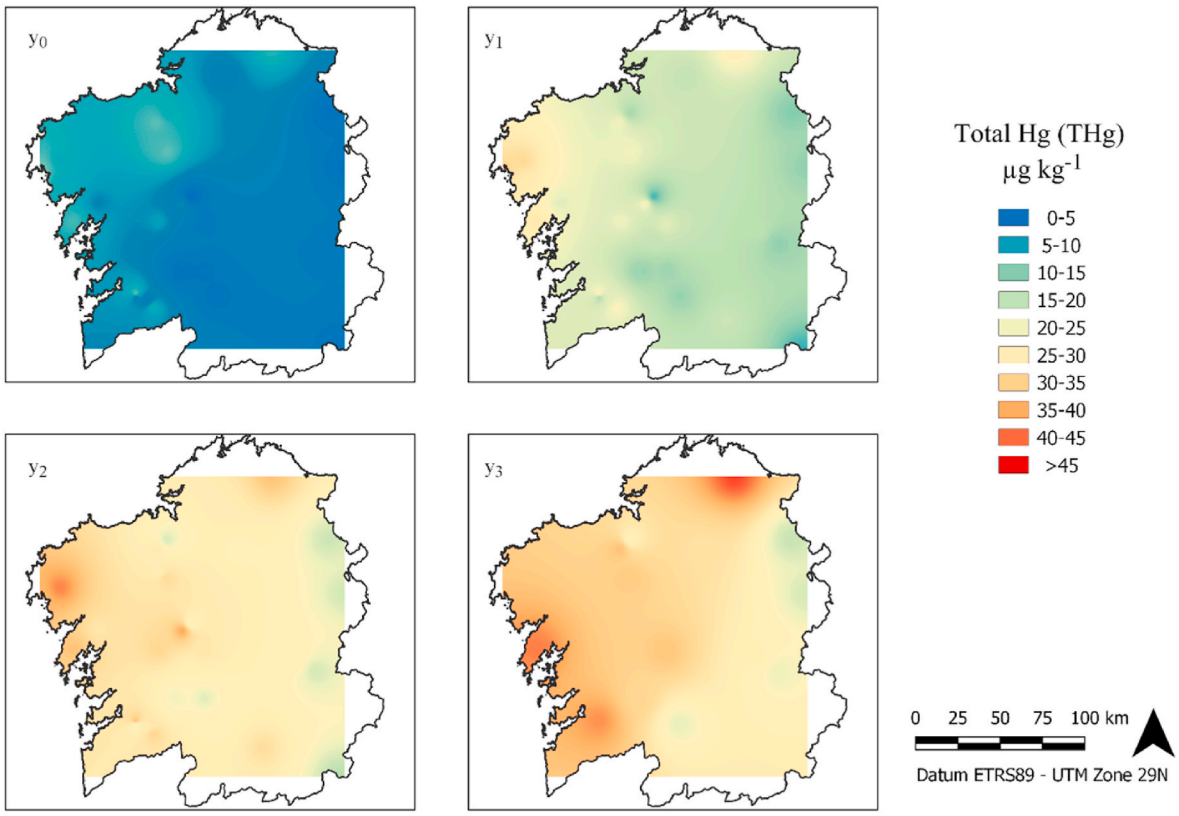

Fig. 2. Spatial variation of the total Hg concentration in *Pinus pinaster* needles depending on age class (y_0, y_1, y_2 and y_3) across Galicia (NW Iberian Peninsula).

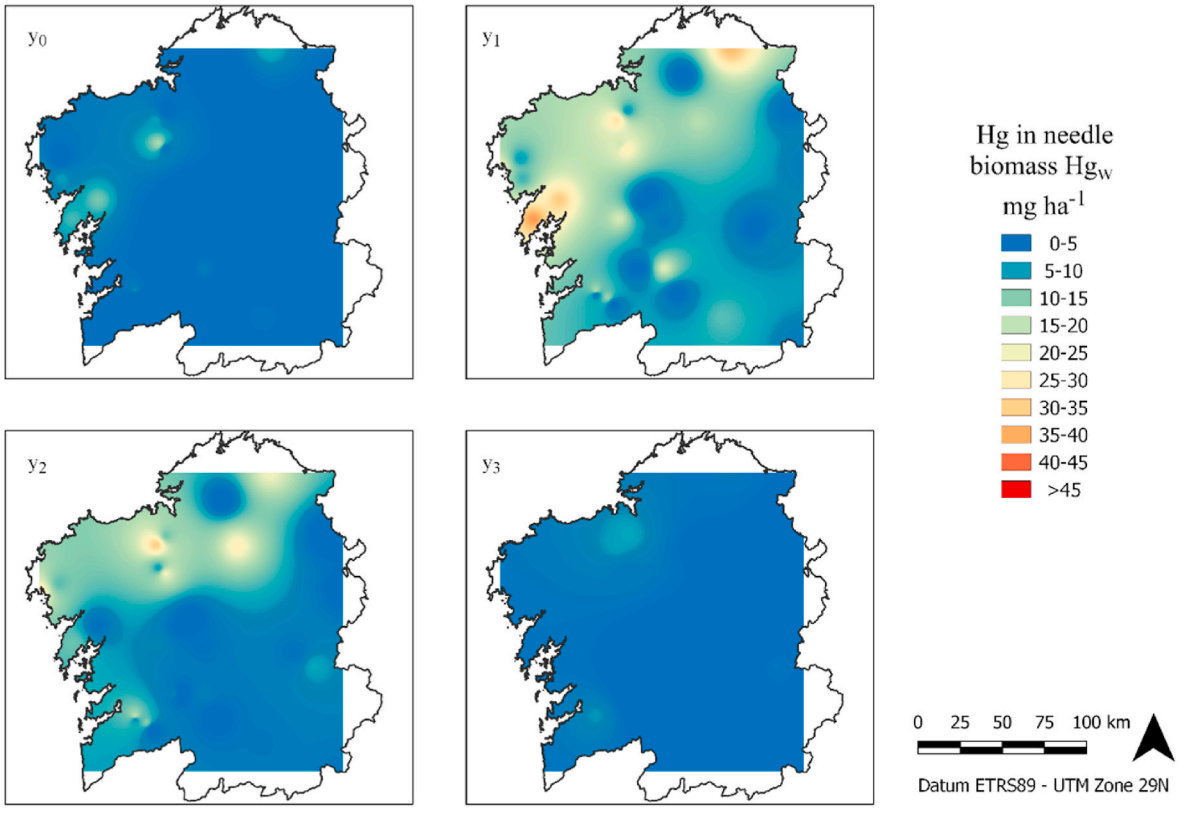

Fig. 3. Spatial variation of total Hg stored in *Pinus pinaster* needles (Hg_W) depending on age class (y_0, y_1, y_2 and y_3) across Galicia (NW Iberian Peninsula).

classes and with respect to the final Hg concentration (i.e. mean THg registered in y_3 needles), y_0 needles accumulated 28% of the final THg, while y_1 needles accumulated 40% of the final THg. The percentage of Hg accumulated by y_2 and y_3 needles diminished to 24 and 8%, respectively. The Hg accumulation rate estimated considering jointly y_0, y_1 and y_2 needle age classes (total Hg accumulation rate, Hg_{Rt}) resulted in a mean value of 10.2 ± 2.3 μg Hg kg^{-1} yr^{-1} (range 6.3–15.1). In agreement with THg in needles, a Mann-Whitney test revealed that Hg_{Rt} was significantly higher in coastal than in inland stands (U = 49.5; p = 0.007; n = 31).

3.2. Total Hg stored in needle biomass

The average of Hg stored in the needle biomass per ground area (Hg_{Wx}) ranged from 5.2 mg Hg ha^{-1} in y_0 and y_3 needles to 14.4 mg Hg ha^{-1} in y_1 needles (Table S4), with y_2 needles showing an intermediate value of 10.9 mg Hg ha^{-1}. Needle age class was a significant factor of variation for Hg stored in needle biomass (H = 50.7; p = 0.000; n = 294), although there was not a linear relationship between needle age and Hg stored in its biomass. The mean biomass of y_1 needles in the studied stands (0.62 Mg ha^{-1}) was only 20% higher than that of y_0 needles, however y_1 needles stored in their biomass, on average, 45% of the Hg present in the total needle biomass per stand (Hg_{Wt}). The younger (y_0) and the older (y_3) needles accounted for only 16 and 14% of the Hg stored in total needle biomass, respectively.

At the stand scale (i.e., considering the total needle biomass per stand), Hg_{Wt} varied between 5.6 and 87.8 mg Hg ha^{-1} with a mean value of 32.5 mg Hg ha^{-1} (Table S4). The spatial distribution of pine stands in the study area was a significant factor of variation for Hg_{Wt} (H = 150.8; p = 0.000; n = 294), showing higher Hg_{Wt} values the closer the stands are to the coastline (U = 39; p = 0.001; n = 31). In agreement, stands 2, 4 and 9 had the highest values of Hg_{Wt} (>70 mg Hg ha^{-1}) whereas the lowest values were found in stands 14, 21 and 24 (Hg_{Wt} < 7 mg Hg ha^{-1}). The spatial variation of Hg_{Wx} (Fig. 3) showed a greater accumulation of Hg in the biomass of y_1 and y_2 needles of stands close to coast (Table 1). The highest values of Hg_W (>30 mg Hg ha^{-1}) were expected for y_1 needles in areas at the middle of the west coast and the far north.

3.3. Estimation of Hg deposition fluxes through needle litterfall

The mean value of the estimated total litterfall flux per stand (L_t) was 0.50 Mg ha^{-1} yr^{-1} (ranging from 0.06 to 2.51 Mg ha^{-1} yr^{-1}; Online Data Resource). Considering the L_t values, the average estimated Hg deposition flux through litterfall per stand (Hg_{Lt}) was 1.54 μg m^{-2} yr^{-1}, with a wide range of variation from 0.18 μg m^{-2} yr^{-1} in the stand 21 to 7.81 μg m^{-2} yr^{-1} in the stand 4 (Table S5). As for THg and Hg_{Wt}, the values of Hg_{Lt} were significantly higher in the stands closer to coastal areas (U = 67.000; p = 0.045; n = 31), being observed the highest Hg_{Lt} in stands 3 and 4 (Table S5).

As expected, the estimated fluxes of Hg deposition through litterfall differed significantly depending on needle age class (H = 156.803; p = 0.000; n = 294). As needles get older, Hg_{Lx} (in μg Hg m^{-2} yr^{-1}) increased following the sequence: y_0 (mean 0.03; range 0.00–0.24) > y_1 (mean 0.18; range 0.01–0.82) > y_2 (mean 0.90; range 0.00–7.27) > y_3 (mean 1.01; range 0.00–3.20). The abscission of the oldest needles (y_2 and y_3) contributed up to 95% of the total Hg deposition flux through litterfall (57 and 38% for y_2 and y_3 needles, respectively).

The spatial variation of Hg_{Lx} showed a certain homogeneity throughout the territory in the case of younger needles (y_0 and y_1), with a Hg deposition mostly below 0.15 μg Hg m^{-2} yr^{-1} (Fig. 4). The percentage of needle survival for these age classes is >88% (Online Data Resource), so y_0 and y_1 needles scarcely contributed to Hg deposition through litterfall. For y_2 needles, the higher values of Hg_{Lt} occurred along a strip that runs parallel to the western coast of Galicia, including a 'hot spot' with an estimated deposition of Hg > 5 μg Hg m^{-2} yr^{-1}

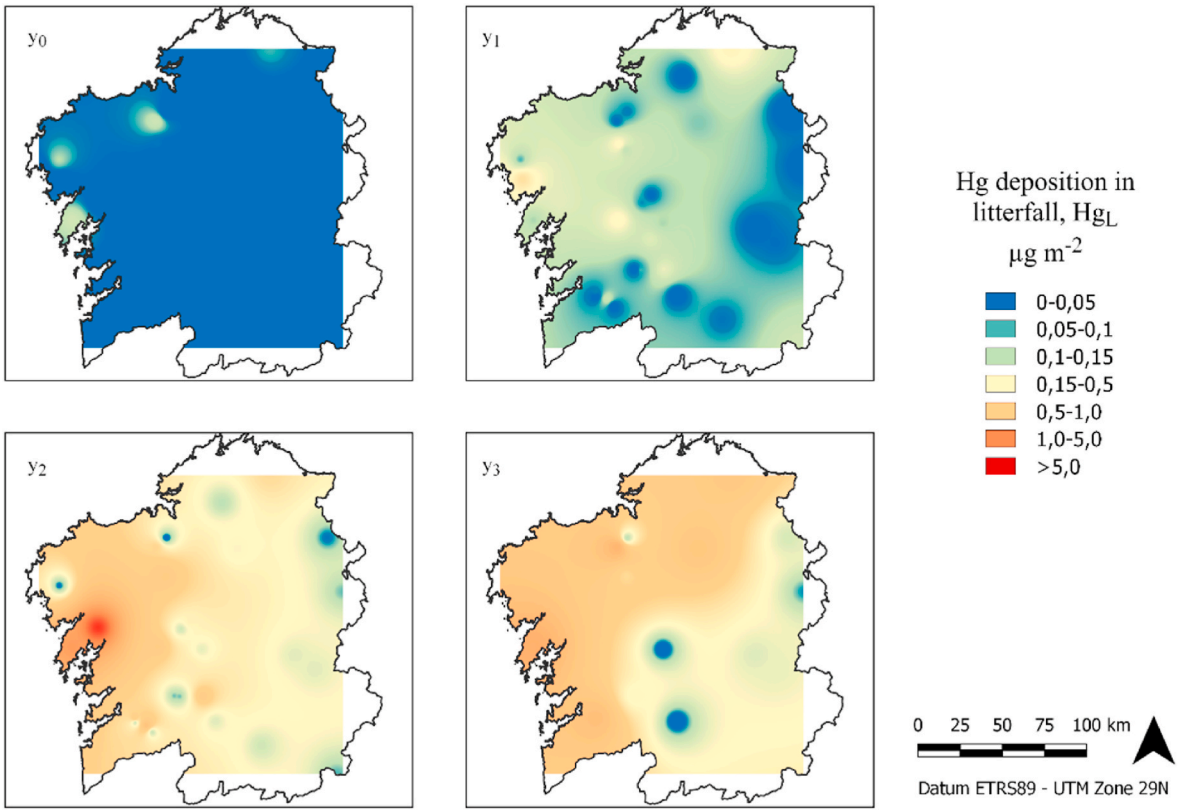

Fig. 4. Spatial variation of annual Hg deposition through litterfall in *Pinus pinaster* needles (Hg_{Lt}) depending on needle age class (y_0, y_1, y_2 and y_3) across Galicia (NW Iberian Peninsula).

(Fig. 4). A spatial gradient in Hg deposition by litterfall between coastal and inland areas appears more clearly for y_3 needles, although no increase in Hg deposition occurs compared to y_2 needles. In fact, values of Hg_L for y_2 and y_3 needle age classes did not differ significantly (U = 922.500; p = 0.302; n = 108).

4. Discussion

4.1. Variations in pine needle Hg concentration

The average of THg in needles of *Pinus pinaster* in the thirty-one stands assessed in this study (21 μg kg^{-1}) is similar to that reported for evergreen needleleaf species (27 μg kg^{-1}) in background locations worldwide (Zhou and Obrist, 2021), suggesting that the study area is not influenced by anthropogenic point sources of Hg emission. However, comparisons of THg in foliage (leaves or needles) should be done with caution, as they may vary among tree species in temperate forests (Obrist et al., 2012; Richardson and Friedland, 2015; Blackwell and Driscoll, 2015b; Navrátil et al., 2016).

In SW Europe, Barghigiani et al. (1991) reported a higher mean value of THg (103 μg kg^{-1}) in *P. pinaster* y_1 needles compared to our data, although their samples were collected in an urban environment. In contrast, Aboal et al. (2004) reported lower THg values in *P. pinaster* needles (mean 12 μg kg^{-1}, range 6–32 μg kg^{-1}) in a study conducted in Galicia (NW Iberian Peninsula), maybe due to the collection of newly sprouted needles as well as their washing before Hg determination. In general, our THg values in needles of the *P. pinaster* (range 3–57 μg kg^{-1}) are comparable to those obtained worldwide in species belonging to the genus *Pinus* (Table 2). However, THg values above 60 μg kg^{-1} were reported in needles of *Pinus* species when the sampling was carried out close to Hg emission point sources such as Hg mines, coal-fired power plants or chlor-alkali factories (Table 2).

The increase of THg with needle age in *P. pinaster* is consistent with the influence of the length of the period of needle exposure to air masses, which was also reported for other coniferous species (Hutnik et al., 2014; Blackwell and Driscoll, 2015a; Navrátil et al., 2017, 2019; Turkyilmaz et al., 2018; Kang et al., 2019; Wohlgemuth et al., 2020). The doubling of THg values in y_1 needles compared to y_0 needles may have been due to the increase of physiological activity just after needle sprouting (Mediavilla and Escudero, 2003), a characteristic observed in other coniferous species (Hutnik et al., 2014; Blackwell and Driscoll, 2015a, b; Wohlgemuth et al., 2020). In addition, greater mean values of leaf area index (LAI) in y_0 and y_1 needles than in y_2 and y_3 ones (Online Data Resource) would justify the higher Hg accumulation rates (Hg_R) observed in the younger needles, which is related to more efficient uptake of atmospheric Hg(0) (Blackwell et al., 2014; Wohlgemuth et al., 2020).

The levelling off of THg with needle age, as shown in y_2 and y_3 needles, is in agreement with the diminution of their Hg_R (Table 1) and in turn, with the decline in the photosynthetic rate with needle ageing (Warren, 2006; Wohlgemuth et al., 2020). The link between the photosynthetic rate and needle age may explain why *P. pinaster* needles uptake, during the first two growing seasons, is about 66% of the THg accumulated at the end of their lifespan.

Mean Hg accumulation rate (Hg_{Rt}) in needles from y_0 to y_2 was 10.2 ± 2.3 μg Hg kg^{-1} yr^{-1}, which is in the range 4–15 μg Hg kg^{-1} yr^{-1} reported in needles of different coniferous species in Europe and the US (Blackwell and Driscoll, 2015a; Navrátil et al., 2019). These similarities in Hg_{Rt} may be justified by a certain homogeneity in atmospheric Hg(0) levels at a hemispheric scale (Navrátil et al., 2019).

Regarding the representation of the spatial variation of THg (Fig. 2), a significant negative correlation was found between THg in pine needles and the distance separating pine stands and the Atlantic Ocean coast (ρ = −0.718; p = 0.000; n = 31 for y_0 needles; ρ = −0.644; p = 0.013; n

Table 2
Comparison of total Hg concentrations in needles of different age from species of genus *Pinus* in this study and in other regions worldwide.

Country	Species	Age classes[a] (yr^{-1})	Mean Hg (μg kg^{-1})	Range Hg (μg kg^{-1})	Reference
Spain	P. pinaster	y_0, y_1, y_2, y_3	21 ± 11	4.3–50.6	this study
	P. pinaster	n.d.	12 ± 6	6.0–32.0	Aboal et al. (2004)
Switzerland	*P. sp.*	y_0, y_1	7 ± 1, 13 ± 3	6.5–13.2	Wohlgemuth et al. (2020)
Poland	P. sylvestris	y_1	11 ± 3	3.2–18.0	Woś et al. (2021)
Russia	P. sylvestris	n.d.		6.0–19.0	Afanasieva et al. (2007)
	P. sylvestris	y_0, y_1, y_2, y_3, y_4	14	8.0–15.0	Lyapina (2018)
Czech Republic	P. sylvestris	y_0, y_1, y_2		19.2–40.9	Navrátil et al. (2017)
	P. sylvestris	y_0	16 ± 6	12.1–20.6	Navrátil et al. (2014)
Norway	*P. sp.*	y_0, y_1	16, 31		Larssen et al. (2008)
Turkey	P. sylvestris	y_0, y_1, y_2	48 ± 9	39.5–56.6	Turkyilmaz et al. (2018)
China	P. tabuliformis	n.d.	45 ± 4		Zhou et al. (2017)
USA	*P. sp.*	n.d.	13		Tabatchnick et al. (2012)
	P. resinosa	y_0, y_1	18 ± 7	8.3–28.3	Fleck et al. (1999)
	P. nigra	y_0, y_1, y_2		42.4–121	
	P. nigra	y_0, y_1, y_2	19 ± 7	9.3–28.8	Hutnik et al. (2014)
	P. resinosa	y_0, y_1	5 ± 2, 18 ± 3		Blackwell and Driscoll (2015a, 2015b)
	P. strobus	y_0, y_1	6 ± 1, 23 ± 4		
	P. jeffreyi	n.d.	23 ± 6	19.0–30.0	Obrist et al. (2011)
	P. jeffreyi	n.d.	15 ± 4	11.2–18.9	Obrist et al. (2009)
	P. strobus	n.d.		13.1–15.5	Yang et al. (2018)
Canada	P. banksiana	n.d.	14.1		Hall and St Louis (2004)
Spain	P.sylvestris	n.d.	60*		Nóvoa-Muñoz et al. (2008)
	P. pinea	n.d.	332*	200-570*	Barquero et al. (2019)
Czech Republic	P. sylvestris	y_0, y_1		61.5–98.0*	Navrátil et al. (2017)
Italy	P. pinaster	y_1	103*		Barghigiani et al. (1991)
	P. sylvestris	y_1	92*		
	P. nigra	y_1	83*		
	P. halepensis	y_1	63*		
	P. pinea	y_1	56*		
China	P. massoniana	n.d.	98*	63-139*	Du et al. (2019)

*Mean values or ranges of Hg accompanied by this symbol mean that samples were collected in areas close to Hg emission point sources such as coal fired power plants, dense populated cities, mine areas, etc.

[a] y_0 means needles sprouted in the sampling year, whereas y_1, y_2 … correspond to subsequent years (n.d. means that needle age is not defined).

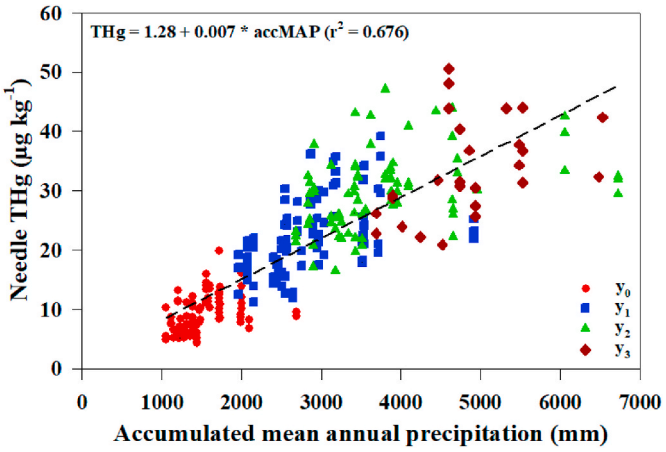

Fig. 5. Relationship between total Hg in pine needles by age class (y_0, y_1, y_2, y_3) and the accumulated mean annual precipitation (accMAP) along needle lifetime. Age class y_0 corresponds to needles sprouted in the sampling year (2009), while needles y_1, y_2 and y_3 sprouted in 2008, 2007 and 2006, respectively.

= 14 for y_3 needles). In the study area, the increasing distance from the sea shoreline to inland areas is accompanied by a decrease in the mean annual precipitation, a fact linked to the general pattern of atmospheric circulation in southwest Atlantic Europe (De Uña Álvarez, 2001; Souto et al., 2003). In fact, mean annual precipitation accumulated over needle life accounted for 68% of the variance of THg in pine needles (Fig. 5), maintaining a very good agreement when the spatial variation of both parameters was represented (Fig. S1). As a result of the spatial variation of THg, we could identify several areas of environmental concern for their high Hg values along the west and far north coasts of Galicia, particularly for older needle classes (y_2 and y_3). A similar relationship between high precipitation, coastal areas and high THg in tree foliage was reported by Obrist et al. (2011). Marine areas are a natural source of Hg from where it is transported along with water vapor and cloud water deposition to the coastal areas, where it is captured by tree foliage (Peckham et al., 2019).

4.2. Mercury storage in needle biomass

Total Hg stored in the needle biomass (Hg_{Wt}) is of great relevance in the biogeochemical cycling of Hg in forest ecosystems, as a substantial fraction will reach the forest floor by litterfall (Zheng et al., 2016; Wang et al., 2017). The mean value of Hg_{Wt} obtained in *P. pinaster* stands from NW Iberian Peninsula (33 mg Hg ha^{-1}) is comparable to the range (40–50 mg Hg ha^{-1}) reported in coniferous species throughout Europe (Wohlgemuth et al., 2020) and the US (Yang et al., 2018). However, higher values of Hg_{Wt}, ranging from 130 to 431 mg Hg ha^{-1}, were observed in other studies (Obrist et al., 2012; Richardson and Friedland, 2015; Zhou et al., 2017). Such discrepancies in Hg_{Wt} could be attributed to species-specific differences in morphological and physiological traits such as roughness, specific leaf area, leaf age or stomatal conductance (Obrist et al., 2012; Blackwell and Driscoll, 2015b; Wohlgemuth et al., 2020) and to climatic conditions that determine foliage biomass production (Wang et al., 2019a; Zhou and Obrist, 2021).

Different factors influenced Hg storage in the needle biomass of each age class (Hg_W), including the amount of needle biomass and the length of needle exposure to air masses and precipitation. The latter factor, given its shortness, justified the low values of Hg_W found in y_0 needles, while in the case of y_3 needles, the low Hg_W was due to the scarcity of needles belonging to this age class, accounting on average for only 10% of the total needle biomass (W_t) in the studied stands (Online Data Resource). On the other hand, the higher values of Hg_W reported for y_1 and y_2 needles resulted from the combination of long enough exposure time to uptake atmospheric Hg(0), as well as their substantial contribution to total needle biomass (40 and 23% for y_1 and y_2 needles, respectively). The Hg_W variation observed in the present study among needle age classes confirms the relevance of needle age in obtaining an accurate estimation of the Hg pool in coniferous foliage (Blackwell and Driscoll, 2015a; Luo et al., 2016; Wohlgemuth et al., 2020).

Higher Hg_{Wt} values in stands closer to coastal areas agree with the significant higher total needle biomass (W_{tn}) reported in them (Online Data Resource), compared to inland stands ($U = 45.0$; $p = 0.003$; $n = 31$). Considering that W_{tn} and mean annual precipitation in the study area are strongly related (Álvarez-Álvarez et al., 2011; Eimil-Fraga et al., 2015a), we hypothesize that the influence of rainfall in the production of biomass is reflected by higher values of Hg_{Wt} in coastal stands. The link between Hg_W and the accumulated mean annual precipitation is clearly seen in the spatial representation of both parameters together, especially for y_1 needles (Fig. S2). Recent findings have highlighted that precipitation strongly influences the net primary production, favouring indirectly a greater atmospheric Hg(0) uptake by plant tissues (Wang et al., 2019a, b; Zhou and Obrist, 2021).

4.3. Mercury deposition through pine needle litterfall

Indirect estimations of Hg deposition through needle litterfall (Hg_{Lt}), which ranged from 0.2 to 7.8 µg Hg m^{-2} yr^{-1}, were lower than the empirical data (14.2–21.1 µg Hg m^{-2} yr^{-1}) obtained in the study area for deciduous and coniferous stands (Gómez-Armesto et al., 2020; Parente-Sendín, 2021). The EMEP predictions for total Hg deposition in coniferous forests in the NW of the Iberian Peninsula are in the range of 10–20 µg Hg m^{-2} yr^{-1} (Strizhkina et al., 2021), also greater than Hg_{Lt} values estimated in the present study. Compared to other areas worldwide, our Hg_{Lt} values are an order of magnitude lower than those reported in coniferous forests from North America (3.0–25.8 µg Hg m^{-2} yr^{-1}) (Louis et al., 2001; Sheehan et al., 2006; Juillerat et al., 2012; Obrist et al., 2012; Richardson and Friedland, 2015; Risch et al., 2017; Gerson et al., 2017) and central and northern Europe (15–45 µg Hg m^{-2} yr^{-1}) (Lee et al., 1998; Schwesig and Matzner, 2000; Navrátil et al., 2019). In summary, the low Hg_{Lt} calculated in the current study could be underestimated due to their indirect quantification based on needle survival rate (S; see Online Data Resource). Moreover, several plant tissues other than needles may contribute to Hg deposition through litterfall (Navrátil et al., 2019; Gómez-Armesto et al., 2020). More accurate estimations of Hg_{Lt} in the study area could be obtained by conducting an assessment based on the deployment of traditional litterfall collectors in the field and determining Hg in the fallen biomass.

The flux of Hg deposition by needle litterfall (Hg_{Lt}) was better correlated with litterfall biomass (L_t) ($\rho = 0.991$; $p = 0.000$; $n = 294$) than with total Hg concentration in needles ($\rho = 0.782$; $p = 0.000$; $n = 294$). Previous studies have already shown that Hg deposition fluxes by litterfall were more influenced by the biomass of litterfall than by the concentration of Hg (Zhou et al., 2013; Wang et al., 2016b; Risch et al., 2017; Gómez-Armesto et al., 2020; Li et al., 2022). The greater values of Hg_{Lt} in the stands closer to coastal areas coincides with those that presented higher total needle biomass (W_t) and, consequently, a greater amount of litterfall biomass (L_t). In addition, given the influence of rainfall on total needle biomass (W_t), a good agreement between accumulated mean annual precipitation and Hg_{Lt} was observed across the study area (Fig. S3). In this sense, a band is traced from the west and north coast of Galicia, where the highest levels of accumulated mean annual precipitation and Hg_{Lt} were reported, with a better definition of the band as needles get older. A similar spatial correlation between Hg_{Lt} and rainfall was attributed to the stimulating effect of precipitation on the production of foliar biomass and, consequently, its contribution to Hg deposition through litterfall (Zheng et al., 2016; Wang et al., 2019b; Li et al., 2022).

The increase in Hg_{Lt} with needle ageing is reasonable considering that y_2 and y_3 needles, which are more prone to fall due to their

upcoming senescence, remain longer active in atmospheric Hg(0) uptake. In this regard, y_2 and y_3 needles contributed between 3 and 14 times more than younger needles (y_0 and y_1) to the total litterfall biomass (L_t) and in turn to the Hg deposition by litterfall. The lack of a spatial pattern in Hg deposition through litterfall for y_0 needles is well justified given their scarce contribution to Hg_{Lt}. In the case of y_2 and y_3 needles, the observed spatial variation of Hg_{Lt} could be related to the effects of strong rainy and windy events that typically occur in coastal areas of oceanic regions (such as Galicia), which would favor needles shedding.

In a scenario in which climatic change would expand the extent of *P. pinaster* forests in Spain (Barrio-Anta et al., 2020), Hg deposition through litterfall is expected to increase in parallel with greater biomass production. In consequence, the ability of soils to retain Hg can be exceeded, threatening its role as Hg sink and triggering Hg toxicity risks to soil wildlife and freshwater ecosystems, as Hg exported in forest runoff comes mainly from foliar uptake of atmospheric Hg(0) (Jiskra et al., 2017). The present findings on spatial distribution and storage of THg in pine needles and its relationship with precipitation, will help to locate concerning areas where further studies (Hg deposition by throughfall, litterfall, atmospheric Hg(0) monitoring, etc.) should be conducted, both on a regional scale and along the Western European Atlantic coastal area.

Furthermore, *Pinus pinaster* forests are a valuable economic resource in the study area (Álvarez-Álvarez et al., 2011), so management plans should include practices that minimize the risk of downstream mobilization of Hg, which is often reported during logging (Kronberg et al., 2016; Bishop et al., 2020). In addition, given the extremely high vulnerability of southwest Europe to forest fires (Turco et al., 2019), the accumulation of pine needles on the forest floor would be regarded as a source of Hg in the case of wildfire (Zhou et al., 2017), and these impacts on Hg cycling in forest ecosystems should be considered (Campos et al., 2015; Kumar et al., 2018).

5. Conclusions

According to the mean total Hg concentration in *Pinus pinaster* needles (21 ± 11 μg Hg kg^{-1}), the NW of the Iberian Peninsula (Galicia, Spain) seems to be exempt from the effects of regional anthropogenic Hg emission point sources. The increase of THg in needles with age was consistent with the length of exposure time to air masses, whereas Hg accumulation rate decreased with needle age probably due to a lesser photosynthetic activity in older needles. The spatial variation of THg in pine needles across NW of the Iberian Peninsula agrees with regional climatic features such as humidity and precipitation, leading to the highest Hg concentrations in needles of coastal pine stands. Monitoring of Hg contents in maritime pine needles of different ages resulted in a useful tool to trace the atmospheric Hg pollution in the study area.

Although Hg storage in *P. pinaster* needle biomass (Hg_{Wt}) was similar to that reported for coniferous species worldwide, needle age and climatic characteristics (accumulated mean annual precipitations) were shown as influencing factors in the estimation of Hg_{Wt}, and its spatial variation. Thus, these factors should be taken into account in future studies evaluating Hg pools in the foliage of coniferous forests.

Mercury deposition through litterfall (Hg_{Lt}) resulted in low values, suggesting that its indirect estimation using the percentage of needle survival (S) could be underestimating the fluxes of Hg deposition. In addition, to the Hg deposition flux from needle fall, we should add the flux corresponding to other plant tissues that are also key in the transfer of Hg from vegetation to the forest soil. In spite of this fact, the obtained values of Hg_{Lt} also showed differences depending on needle age class as well as climatic characteristics. Thus, frequent rainy and windy events in coastal areas would favor the fall of older needles increasing Hg_{Lt} fluxes in the stands closer to the sea shoreline as it was observed in its spatial representation.

The scavenging of atmospheric Hg(0) by pine needles, the dynamics of its storage in the biomass and transference to soil surface could be easily modified due to global warming and land use changes. These variations can affect the role of forest soils as Hg sink in terrestrial ecosystems, leading to concerning environmental consequences that should be addressed.

The results of Hg concentration, accumulation and deposition in pine forests of the NW of the Iberian Peninsula would complete the scarce information provided by EMEP for this region of Europe, helping to improve national actions in accordance with the implementation of the Minamata Convention.

Author statement

Méndez-López, M.: Conceptualization, Methodology, Data Curation, Visualization, Formal analysis, Investigation, Writing- Original Draft, Writing - review & editing. **Gómez-Armesto, A.:** Methodology, Data Curation, Formal analysis, Investigation, Writing- Original Draft, Writing - review & editing. **Eimil-Fraga, Cristina:** Resources, Data Curation, Investigation, Visualization, Writing - review & editing. **Alonso-Vega, Flora:** Writing- Original Draft, Funding acquisition, Resources, Visualization, Supervision, Writing - review & editing. **Rodríguez-Soalleiro, Roque:** Funding acquisition, Data Curation, Investigation, Visualization, Writing - review & editing. **Álvarez-Rodríguez, Esperanza:** Funding acquisition, Data Curation, Investigation, Visualization, Writing - review & editing. **Arias-Estévez, Manuel:** Funding acquisition, Visualization, Resources, Supervision, Project administration. **Nóvoa-Muñoz, Juan Carlos:** Conceptualization, Formal analysis, Visualization, Resources, Writing- Original Draft, Supervision, Writing - review & editing, Funding acquisition, Project administration.

Declaration of competing interest

The authors declare that they have no known competing financial interests or personal relationships that could have appeared to influence the work reported in this paper.

Data availability

Data will be made available on request.

Acknowledgments

M. Méndez-López acknowledges the predoctoral grant FPU of Ministerio de Educación y Formación Profesional (FPU17/05484). The valuable collaboration of MSc. Aitor Freire Astray is also very appreciated during the application of GIS tools to represent the spatial variation of Hg. It is also recognized the financial support of Consellería de Cultura, Educación e Universidade (Xunta de Galicia) through the contract ED431C 2021/46-GRC granted to the research group BV1 of the University of Vigo and the research projects ED431F2018/06-EXCELENCIA and ED431C2018/07. This research has received funding for open access charge by Universidade de Vigo/CISUG.

Appendix A. Supplementary data

Supplementary data related to this article can be found at https://doi.org/10.1016/j.envres.2022.114223.

References

Aboal, J.R., Fernández, J.A., Carballeira, A., 2004. Oak leaves and pine needles as biomonitors of airborne trace elements pollution. Environ. Exp. Bot. 51, 215–225.
Afanasieva, L.V., Kashin, V.K., Mikhailova, T.A., Berezhnaya, N.S., 2007. Effect of the industry-related air pollution on the accumulation of heavy metals in the pine needles in the basin of the Selenga River. Chem. Sustain. Dev. 15, 25–31.

Álvarez-Álvarez, P., Khouri, E.A., Cámara-Obregón, A., Castedo-Dorado, F., Barrio-Anta, M., 2011. Effects of foliar nutrients and environmental factors on site productivity in *Pinus pinaster* Ait. stands in Asturias (NW Spain). Ann. For. Sci. 68, 497–509.

Arnold, J., Gustin, M.S., Weisberg, P.J., 2018. Evidence for nonstomatal uptake of Hg by aspen and translocation of Hg from foliage to tree rings in Austrian pine. Environ. Sci. Technol. 52 (3), 1174–1182.

Barghigiani, C., Ristori, T., Bauleo, R., 1991. Pinus as an atmospheric Hg biomonitor. Environ. Technol. 12, 1175–1181.

Barrio-Anta, M., Castedo-Dorado, F., Cámara-Obregón, A., López-Sánchez, C.A., 2020. Predicting current and future suitable habitat and productivity for Atlantic populations of maritime pine (*Pinus pinaster* Aiton) in Spain. Ann. For. Sci. 77 (2), 1–19.

Bishop, K., Shanley, J.B., Riscassi, A., de Wit, H.A., Eklöf, K., Meng, B., Mitchell, C., Osterwalder, S., Schuster, P.F., Webster, J., Zhu, W., 2020. Recent advances in understanding and measurement of mercury in the environment: terrestrial Hg cycling. Sci. Total Environ. 721, 137647.

Blackwell, B.D., Driscoll, C.T., 2015a. Deposition of mercury in forests along a montane elevation gradient. Environ. Sci. Technol. 49, 5363–5370.

Blackwell, B.D., Driscoll, C.T., 2015b. Using foliar and forest floor mercury concentrations to assess spatial patterns of mercury deposition. Environ. Pollut. 202, 126–134.

Blackwell, B.D., Driscoll, C.T., Maxwell, J.A., Holsen, T.M., 2014. Changing climate alters inputs and pathways of mercury deposition to forested ecosystems. Biogeochemistry 119, 215–228.

Barquero, J.I., Rojas, S., Esbrí, J.M., García-Noguero, E.M., Higueras, P., 2019. Factors influencing mercury uptake by leaves of stone pine (*Pinus pinea* L.) in Almadén (Central Spain). Environ. Sci. Pollut. Res. 26 (4), 3129–3137.

Campos, I., Vale, C., Abrantes, N., Keizer, J.J., Pereira, P., 2015. Effects of wildfire on mercury mobilisation in eucalypt and pine forests. Catena 131, 149–159.

Coale, K., Heim, W., Negrey, J., Weiss-Penzias, P., Fernandez, D., Olson, A., Chiswell, H., Byington, A., Bonnema, A., Martenuk, S., 2018. The distribution and speciation of mercury in the California current: implications for mercury transport via fog to land. Deep Sea Res. Part II Top. Stud. Oceanogr. 151, 77–88.

De Uña Álvarez, E., 2001. El clima. In: Precedo Ledo, A., Sancho Comíns, J. (Eds.), Atlas de Galicia. Tomo 1: Medio Natural, Sociedade para o Desenvolvemento Comarcal de Galicia, Xunta de Galicia.

Demers, J.D., Blum, J.D., Zak, D.R., 2013. Mercury isotopes in a forested ecosystem: implications for air-surface exchange dynamics and the global mercury cycle. Global Biogeochem. Cycles 27, 222–238.

Driscoll, C.T., Mason, R.P., Chan, H.M., Jacob, D.J., Pirrone, N., 2013. Mercury as a global pollutant: sources, pathways, and effects. Environ. Sci. Technol. 47, 4967–4983.

Du, B., Zhou, J., Zhou, L., Fan, X., Zhou, J., 2019. Mercury distribution in the foliage and soil profiles of a subtropical forest: process for mercury retention in soils. J. Geochem. Explor. 205, 106337.

EEA, 2017. Climate Change, Impacts and Vulnerability in Europe 2016. An Indicator-Based Report. European Environment Agency Report N° 1/2017.

Eimil-Fraga, C., Sánchez-Rodríguez, F., Álvarez-Rodríguez, E., Rodríguez-Soalleiro, R., 2015a. Relationships between needle traits, needle age and site and stand parameters in *Pinus pinaster*. Trees (Berl.) 29, 1103–1113.

Eimil-Fraga, C., Sánchez-Rodríguez, F., Álvarez-Rodríguez, E., Rodríguez-Soalleiro, R., 2015b. Variability in needle lifespan and foliar biomass along a gradient of soil fertility in maritime pine plantations on acid soils rich in organic matter. For. Ecol. Manage. 343, 34–41.

Fleck, J.A., Grigal, D.F., Nater, E.A., 1999. Mercury uptake by trees: an observational experiment. Water, Air, Soil Pollut. 115 (1), 513–523.

Fortin, M.J., Dale, M., 2005. Spatial Analysis. A Guide for Ecologists. Cambridge University Press.

Forzieri, G., Girardello, M., Ceccherini, G., Spinoni, J., Feyen, L., Hartmann, H., Beck, P. S.A., Camps-Valls, G., Chirici, G., Mauri, A., Cescatti, A., 2021. Emergent vulnerability to climate-driven disturbances in European forests. Nat. Commun. 12 (1), 1–12.

Gerson, J.R., Driscoll, C.T., Demers, J.D., Sauer, A.K., Blackwell, B.D., Montesdeoca, M. R., Shanley, J.B., Ross, D.S., 2017. Deposition of mercury in forests across a montane elevation gradient: elevational and seasonal patterns in methylmercury inputs and production. J. Geophys. Res. Biogeosci. 122, 1922–1939.

Gómez-Armesto, A., Méndez-López, M., Pérez-Rodríguez, P., Fernández-Calviño, D., Arias-Estévez, M., Nóvoa-Muñoz, J., 2020. Litterfall Hg deposition to an oak forest soil from southwestern Europe. J. Environ. Manag. 269, 110858.

Hall, B.D., St. Louis, V.L., 2004. Methylmercury and total mercury in plant litter decomposing in upland forests and flooded landscapes. Environ. Sci. Technol. 38 (19), 5010–5021.

Hararuk, O., Obrist, D., Luo, Y., 2013. Modelling the sensitivity of soil mercury storage to climate-induced changes in soil carbon pools. Biogeosciences 10, 2393–2407.

Hevia, A., Crabiffosse, A., Álvarez-González, J.G., Ruiz-González, A.D., Majada, J., 2017. Novel approach to assessing residual biomass from pruning: a case study in Atlantic *Pinus pinaster* Ait. timber forests. Renew. Energy 107, 620–628.

Hutnik, R.J., McClenahen, J.R., Long, R.P., Davis, D.D., 2014. Mercury accumulation in *Pinus nigra* (Austrian pine). Northeast. Nat. 21, 529–540.

Jiskra, M., Wiederhold, J.G., Skyllberg, U., Kronberg, R.M., Kretzschmar, R., 2017. Source tracing of natural organic matter bound mercury in boreal forest runoff with mercury stable isotopes. Environ. Sci.: Process. Impacts 19, 1235–1248.

Juillerat, J.I., Ross, D.S., Bank, M.S., 2012. Mercury in litterfall and upper soil horizons in forested ecosystems in Vermont, USA. Environ. Toxicol. Chem. 31, 1720–1729.

Kang, H., Liu, X., Guo, J., Wang, B., Xu, G., Wu, G., Kang, S., Huang, J., 2019. Characterization of mercury concentration from soils to needle and tree rings of Schrenk spruce (*Picea schrenkiana*) of the middle Tianshan Mountains, northwestern China. Ecol. Indicat. 104, 24–31.

Kronberg, R., Drott, A., Jiskra, M., Wiederhold, J.G., Björn, E., Skyllberg, U., 2016. Forest harvest contribution to Boreal freshwater methyl mercury load. Global Biogeochem. Cycles 30, 825–843.

Kumar, A., Wu, S., Huang, Y., Liao, H., Kaplan, J.O., 2018. Mercury from wildfires: global emission inventories and sensitivity to 2000–2050 global change. Atmos. Environ. 173, 6–15.

Laacouri, A., Nater, E.A., Kolka, R.K., 2013. Distribution and uptake dynamics of mercury in leaves of common deciduous tree species in Minnesota. U.S.A. Environ. Sci. Technol. 47, 10462–10470.

Larssen, T., de Wit, H.A., Wiker, M., Halse, K., 2008. Mercury budget of a small forested boreal catchment in southeast Norway. Sci. Total Environ. 404 (2–3), 290–296.

Lee, Y., Bishop, K., Munthe, J., Verta, M., Parkman, H., Hultberg, H., 1998. An examination of current Hg deposition and export in Fenno-Scandian catchments. Biogeochemistry 40, 125–135.

Li, X., Wang, X., Yuan, W., Lu, Z., Wang, D., 2022. Increase of litterfall mercury input and sequestration during decomposition with a montane elevation in Southwest China. Environ. Pollut. 292, 118449.

Louis, V.L.S.T., Rudd, J.W.M., Kelly, C.A., Hall, B.D., Rolfhus, K.R., Scott, K.J., Lindberg, S.E., Dong, W., 2001. Importance of the forest canopy to fluxes of methyl mercury and total mercury to boreal ecosystems. Environ. Sci. Technol. 35, 3089–3098.

Luo, Y., Duan, L., Driscoll, C.T., Xu, G., Shao, M., Taylor, M., Wang, S., Hao, J., 2016. Foliage/atmosphere exchange of mercury in a subtropical coniferous forest in south China. J. Geophys. Res. Biogeosci. 121, 2006–2016.

Lyapina, E., 2018. Dynamics and features of mercury accumulation in coniferous trees of Tomsk region. IOP Conf. Ser. Earth Environ. Sci. 211 (1), 012051.

Mediavilla, S., Escudero, A., 2003. Photosynthetic capacity, integrated over the lifetime of a leaf, is predicted to be independent of leaf longevity in some tree species. New Phytol. 159, 203–211.

Meteogalicia.gal, 2021. Meteogalicia. Concellería de Medio Ambiente. Territorio e Vivenda. Xunta de Galicia. https://www.meteogalicia.gal.

Navrátil, T., Nováková, T., Roll, M., Shanley, J.B., Kopáček, J., Rohovec, J., Kaňa, J., Cudlín, P., 2019. Decreasing litterfall mercury deposition in central European coniferous forests and effects of bark beetle infestation. Sci. Total Environ. 682, 213–225.

Navrátil, T., Shanley, J., Rohovec, J., Hojdová, M., Penížek, V., Buchtová, J., 2014. Distribution and pools of mercury in Czech forest soils. Water, Air, Soil Pollut. 225 (3), 1–17.

Navrátil, T., Shanley, J.B., Rohovec, J., Oulehle, F., Šimecek, M., Houška, J., Cudlín, P., 2016. Soil mercury distribution in adjacent coniferous and deciduous stands highly impacted by acid rain in the Ore Mountains, Czech Republic. Appl. Geochem. 75, 63–75.

Navrátil, T., Šimeček, M., Shanley, J.B., Rohovec, J., Hojdová, M., Houška, J., 2017. The history of mercury pollution near the Spolana chlor-alkali plant (Neratovice, Czech Republic) as recorded by Scots pine tree rings and other bioindicators. Sci. Total Environ. 586, 1182–1192.

Nóvoa-Muñoz, J.C., Pontevedra-Pombal, X., Martinez-Cortizas, A., Gayoso, E.G.R., 2008. Mercury accumulation in upland acid forest ecosystems nearby a coal-fired power-plant in Southwest Europe (Galicia, NW Spain). Sci. Total Environ. 394 (2–3), 303–312.

Obrist, D., Johnson, D.W., Edmonds, R.L., 2012. Effects of vegetation type on mercury concentrations and pools in two adjacent coniferous and deciduous forests. J. Plant Nutr. Soil Sci. 175, 68–77.

Obrist, D., Johnson, D.W., Lindberg, S.E., 2009. Mercury concentrations and pools in four Sierra Nevada forest sites, and relationships to organic carbon and nitrogen. Biogeosciences 6 (5), 765–777.

Obrist, D., Johnson, D.W., Lindberg, S.E., Luo, Y., Hararuk, O., Bracho, R., Battles, J.J., Dail, D.B., Edmonds, R.L., Monson, R.K., Ollinger, S.V., Pallardy, S.G., Pregitzer, K. S., Todd, D.E., 2011. Mercury distribution across 14 U.S. Forests. Part I: spatial patterns of concentrations in biomass, litter, and soils. Environ. Sci. Technol. 45, 3974–3981.

Obrist, D., Roy, E.M., Harrison, J.L., Kwong, C.F., William Munger, J., Moosmüller, H., Romero, C.D., Sun, S., Zhou, J., Commane, R., 2021. Previously unaccounted atmospheric mercury deposition in a midlatitude deciduous forest. Proc. Natl. Acad. Sci. U. S. A 118 (29).

Olaya, V., 2012. Sistemas de Información Geográfica. Tomo I. ©2012 Víctor Olaya.

Parente-Sendín, A., 2021. Contribución de la biomasa senescente de *Pinus sylvestris* a la transferencia de Hg atmosférico al suelo. Bachelor Degree Report. Faculty of Sciences, University of Vigo, Ourense, Spain, p. 79 (in Spanish).

Peckham, M.A., Gustin, M.S., Weisberg, P.J., Weiss-Penzias, P., 2019. Results of a controlled field experiment to assess the use of tree tissue concentrations as bioindicators of air Hg. Biogeochemistry 142, 265–279.

Picos, J., Rodríguez-Soalleiro, R., 2019. Retos para la selvicultura del pino pináster en Galicia. En "Nuevas perspectivas del pino pináster en España". Fundación Hazi Fundazioa, Araba, pp. 37–54.

QGIS.org, 2021. QGIS Geographic Information System. QGIS Association. http://www.qgis.org.

Richardson, J.B., Friedland, A.J., 2015. Mercury in coniferous and deciduous upland forests in northern New England, USA: implications of climate change. Biogeosciences 12, 6737–6749.

Risch, M.R., DeWild, J.F., Gay, D.A., Zhang, L., Boyer, E.W., Krabbenhoft, D.P., 2017. Atmospheric mercury deposition to forests in the eastern USA. Environ. Pollut. 228, 8–18.
Schwesig, D., Matzner, E., 2000. Pools and fluxes of mercury and methylmercury in two forested catchments in Germany. Sci. Total Environ. 260, 213–223.
Sheehan, K.D., Fernandez, I.J., Kahl, J.S., Amirbahman, A., 2006. Litterfall mercury in two forested watersheds at Acadia National Park, Maine, USA. Water Air Soil Pollut. 170, 249–265.
Souto, M.J., Balseiro, C.F., Pérez-Munuzuri, V., Xue, M., Brewster, K., 2003. Impact of cloud analysis on numerical weather prediction in the Galician region of Spain. J. Appl. Meteorol. 42, 129–140.
Strizhkina, I., Ilyin, I., Rozovskaya, O., Travnikov, 2021. Heavy Metals and POPs: Pollution Assessment of Toxic Substances on Regional and Global Scales. Part I. Supplementary Material for Heavy Metals. MSC-E Data report 1/2021. Moscow, Russia.
Tabatchnick, M.D., Nogaro, G., Hammerschmidt, C.R., 2012. Potential sources of methylmercury in tree foliage. Environ. Pollut. 160, 82–87.
Turco, M., Jerez, S., Augusto, S., Tarín-Carrasco, P., Ratola, N., Jiménez-Guerrero, P., Trigo, R.M., 2019. Climate drivers of the 2017 devastating fires in Portugal. Sci. Rep. 9 (1), 1–8.
Turkyilmaz, A., Sevik, H., Cetin, M., 2018. The use of perennial needles as biomonitors for recently accumulated heavy metals. Landsc. Ecol. Eng. 14, 115–120.
UN Environment: Global Mercury Assessment Report, 2018. UN environmental Programme, chemicals and health branch Geneva, Switzerland. available at: https://wedocs.unep.org/.
Wang, X., Luo, J., Yin, R., Yuan, W., Lin, C., Sommar, J., Feng, X., Wang, H., Lin, C., 2017. Using mercury isotopes to understand mercury accumulation in the montane forest floor of the Eastern Tibetan Plateau. Environ. Sci. Technol. 51, 801–809.
Wang, X., Yuan, W., Lin, C., Zhang, L., Zhang, H., Feng, X., 2019a. Climate and vegetation as primary drivers for global mercury storage in surface soil. Environ. Sci. Technol. 53, 10665–10675.
Wang, X., Bao, Z., Lin, C.-., Yuan, W., Feng, X., 2016a. Assessment of global mercury deposition through litterfall. Environ. Sci. Technol. 50, 8548–8557.
Wang, X., Lin, C.-., Lu, Z., Zhang, H., Zhang, Y., Feng, X., 2016b. Enhanced accumulation and storage of mercury on subtropical evergreen forest floor: implications on mercury budget in global forest ecosystems. J. Geophys. Res. Biogeosci. 121, 2096–2109.
Wang, X., Yuan, W., Lu, Z., Lin, C., Yin, R., Li, F., Feng, X., 2019b. Effects of precipitation on mercury accumulation on subtropical montane forest floor: implications on climate forcing. J. Geophys. Res. Biogeosci. 124, 959–972.
Warren, C.R., 2006. Why does photosynthesis decrease with needle age in *Pinus pinaster*? Trees (Berl.) 20, 157–164.
Witt, E.L., Kolka, R.K., Nater, E.A., Wickman, T.R., 2009. Influence of the forest canopy on total and methyl mercury deposition in the boreal forest. Water Air Soil Pollut. 199, 3–11.
Wohlgemuth, L., Osterwalder, S., Joseph, C., Kahmen, A., Hoch, G., Alewell, C., Jiskra, M., 2020. A bottom-up quantification of foliar mercury uptake fluxes across Europe. Biogeosciences 17, 6441–6456.
Woś, B., Gruba, P., Socha, J., Pietrzykowski, M., 2021. Biomonitoring of mercury contamination in Poland based on its concentration in Scots pine (*Pinus sylvestris* L.) foliage. Int. J. Environ. Res. Publ. Health 18 (19), 10366.
Wright, L., Zhang, L., Marsik, F.J., 2016. Overview of mercury dry deposition, litterfall, and throughfall studies. Atmos. Chem. Phys. 16, 13399–13416.
Yang, Y., Meng, L., Yanai, R.D., Montesdeoca, M., Templer, P.H., Asbjornsen, H., Rustad, L.E., Driscoll, C.T., 2019. Climate change may alter mercury fluxes in northern hardwood forests. Biogeochemistry 146 (1), 1–16.
Yang, Y., Yanai, R.D., Driscoll, C.T., Montesdeoca, M., Smith, K.T., 2018. Concentrations and content of mercury in bark, wood, and leaves in hardwoods and conifers in four forested sites in the northeastern USA. PLoS One 13 (4), e0196293.
Zhang, Y., Song, Z., Huang, S., Zhang, P., Peng, Y., Wu, P., Gu, J., Dutkiewicz, S., Zhang, H., Wu, S., Wang, F., Chen, L., Wang, S., Li, P., 2021. Global health effects of future atmospheric mercury emissions. Nat. Commun. 12, 3035.
Zheng, W., Obrist, D., Weis, D., Bergquist, B.A., 2016. Mercury isotope compositions across North American forests. Global Biogeochem. Cycles 30, 1475–1492.
Zhou, J., Du, B., Shang, L., Wang, Z., Cui, H., Fan, X., Zhou, J., 2020. Mercury fluxes, budgets, and pools in forest ecosystems of China: a review. Crit. Rev. Environ. Sci. Technol. 50, 1411–1450.
Zhou, J., Feng, X., Liu, H., Zhang, H., Fu, X., Bao, Z., Wang, X., Zhang, Y., 2013. Examination of total mercury inputs by precipitation and litterfall in a remote upland forest of Southwestern China. Atmos. Environ. 81, 364–372.
Zhou, J., Obrist, D., 2021. Global mercury assimilation by vegetation. Environ. Sci. Technol. 55, 14245–14257.
Zhou, J., Obrist, D., Dastoor, A., Jiskra, M., Ryjkov, A., 2021. Vegetation uptake of mercury and impacts on global cycling. Nat. Rev. Earth Environ. 2, 269–284.
Zhou, J., Wang, Z., Zhang, X., Gao, Y., 2017. Mercury concentrations and pools in four adjacent coniferous and deciduous upland forests in Beijing, China. J. Geophys. Res. Biogeosci. 122, 1260–1274.